B. R. Sutherland[*]

University of Alberta, Edmonton, Canada

1. INTRODUCTION

In continuously stratified fluid, vertically propagating internal gravity waves of moderately large amplitude can become unstable and possibly break due to a variety of mechanisms including parametric subharmonic instability (PSI) and self-acceleration. In parametric subharmonic instability, energy from primary waves is transferred, for example, to waves with half frequency. This mechanism has been studied in simulations and analytic theory for plane periodic primary waves and has been studied in experiments for low modes in a box filled with uniformly stratified fluid. Conversely, self-acceleration refers to a mechanism whereby a wavepacket induces a mean flow (analogous to the Stokes drift of surface waves) which itself advects the waves until they become convectively unstable. Although self-acceleration cannot operate for plane waves or for modes in a box, simulations show that self-acceleration dominates over parametric subharmonic instability if the wavepacket has sufficiently small vertical extent ((Sutherland 2005)).

The point of the work presented here is to examine circumstances under which a wavepacket becomes unstable due to self-acceleration or parametric subharmonic instability as a function of the wavepacket shape and vertical extent.

2. DESCRIPTION OF MODEL

Numerical simulations are performed by solving the fully nonlinear Navier Stokes equations in two dimensions, x and z, and under the Boussinesq approximation. In all simulations, the background stratification is taken to be uniform, so that N^2, the squared buoyancy frequency, is constant.

On this background we superimpose a perturbation corresponding to a horizontally periodic wave with fixed horizontal wavenumber, k_x. The initial vertical structure is prescribed by the product of an envelope with a vertically periodic wave. Explicitly, the vertical displacement field is (the real part of)

$$\xi(x, z, 0) = A_\xi \ \hat{\xi}(z) e^{i(k_x x + k_z z)}, \qquad (1)$$

[*]Dept. Mathematical and Statistical Sciences, U. Alberta, Edmonton, AB T6G 2G1, Canada;
e-mail: bruce.sutherland@ualberta.ca;
web: http://mach.math.ualberta.ca/~bruce

in which k_z is a constant, representing the vertical wavenumber of waves in the wavepacket, A_ξ is a real, positive constant representing the wavepacket amplitude, and $\hat{\xi}$ takes the following general form:

$$\hat{\xi} \equiv \begin{cases} \exp\left(-\frac{(z-L_z)^2}{2\sigma^2}\right) & z > L_z \\ 1 & |z| \leq L_z \\ \exp\left(-\frac{(z+L_z)^2}{2\sigma^2}\right) & z < -L_z \end{cases} . \qquad (2)$$

In the case $L_z = 0$, (2) defines a Gaussian wavepacket with width given by the standard deviation, σ. In cases with $L_z > 0$, the wavepacket structure is said to be "plateau-shaped" and the half-width of the wavepacket is $L_z + \sigma$. Figure 1 presents an example of a plateau-shaped wavepacket.

The focus of this study is on nonhydrostatic waves because it is for these waves that interactions between the waves and the wave-induced mean flow results in instabilities that grow faster than parametric subharmonic instability.

In the simulations there is no initial background horizontal flow except for that predicted to be induced by waves. Explicitly the wave-induced mean flow is given by the correlation of the vertical displacement and vorticity fields:

$$\langle u \rangle = - \langle \xi \zeta \rangle . \qquad (3)$$

A plot of this mean flow is given in Fig. 1c.

While running, the code systematically computes the instantaneous vertical profiles of the mean horizontal velocity and the predicted value of the wave-induced mean flow using eq. (3). As a measure of the stability of the wavepacket to self-acceleration, these are compared with the horizontal group velocity predicted by linear theory

$$c_{gx} = N \frac{k_z^2}{(k_x^2 + k_z^2)^{3/2}} = \frac{N}{k_x} \cos\Theta \sin^2\Theta. \qquad (4)$$

3. RESULTS

Figure 2 which shows the evolution of a narrow Gaussian wavepacket. The amplitude is moderately large in that the half peak-to-peak vertical displacement is almost 5 percent of the horizontal wavelength: $A_\xi/\lambda_x \simeq 0.048$.

The wavepacket is unstable in the sense that its maximum amplitude increases in time. This is consistent with the result of (Sutherland 2001), who
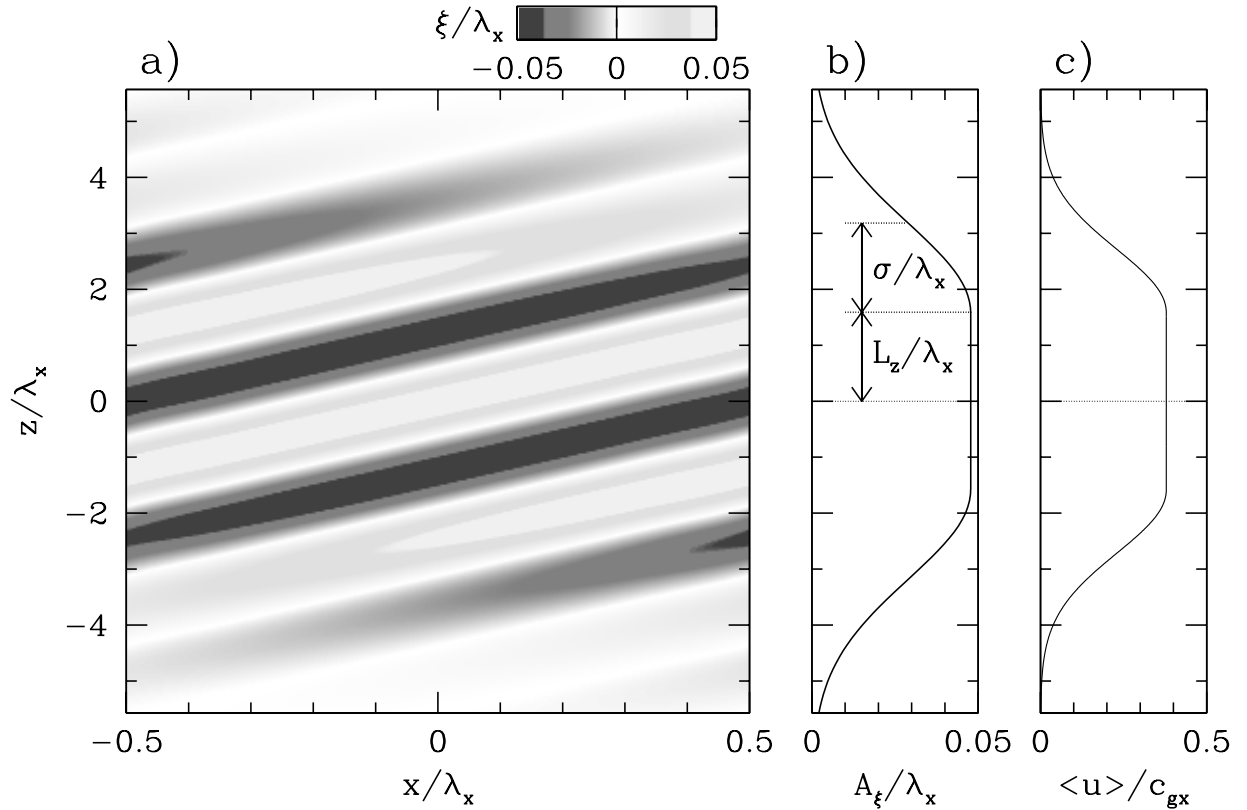
Figure 1: a) Grayscale contours showing vertical displacement field associated with wavepacket at the start of a typical simulation. b) Vertical profile of the associate wave-induced mean flow and Reynolds stress associated with the wavepacket. Parameters are $A_\xi k_x = 0.30$, $k_z/k_x = -0.4$, $L_z k_x = 10$, $\sigma k_x = 10$.

demonstrated that the amplitude envelope of a vertically compact wavepacket increases if its peak frequency is faster than that of waves with the largest vertical group velocity. That is, an amplitude increase is expected if $|k_z| < 2^{-1/2} k_x$.

The speed of the wave-induced mean flow, $\langle u \rangle$, increases as the square of the wavepacket amplitude. In this simulation, Fig. 2d shows that $\langle u \rangle$ increases to almost half the speed of the horizontal group velocity after approximately 8 buoyancy periods ($Nt \simeq 50$). The phase lines near the centre of the wavepacket tilt upward (see Fig. 2b) and the vertical advance of the wavepacket slows.

These dynamics are the result of self-acceleration. Though in this simulation the waves are not of such large amplitude initially that they evolve to overturn and break, the wave-induced mean flow is sufficiently large to advect the waves horizontally at different speeds with height. This implicitly imposed shear is what Doppler-shifts the waves, locally increasing their frequency near the center of the wavepacket.

At still later times the growth of parametrically unstable disturbances becomes evident. After 32 buoyancy periods ($Nt = 200$) small vertical wavelength waves with half the horizontal wavelength of the initial wavepacket have developed beneath the central peak of the wavepacket (Fig. 2c).

The vertical rate of change of the amplitude envelope determines the growth rate of the instability due to self-acceleration. This is demonstrated in Figure 3 which shows the evolution of a large-amplitude Gaussian wavepacket.

The peak amplitude of the wavepacket grows in time but at approximately one quarter the rate. Thus only after approximately 16 buoyancy periods (Fig. 3b) does the vertical tilting of phase lines become evident, and only after approximately 32 buoyancy periods (Fig. 3c) has the relative frequency has been altered to such an extent that the vertical advance of the wavepacket slows (Fig. 3d).

Parametric subharmonic instability, though expected to occur eventually, is not manifest to any significant amplitude by the end of this simulation.
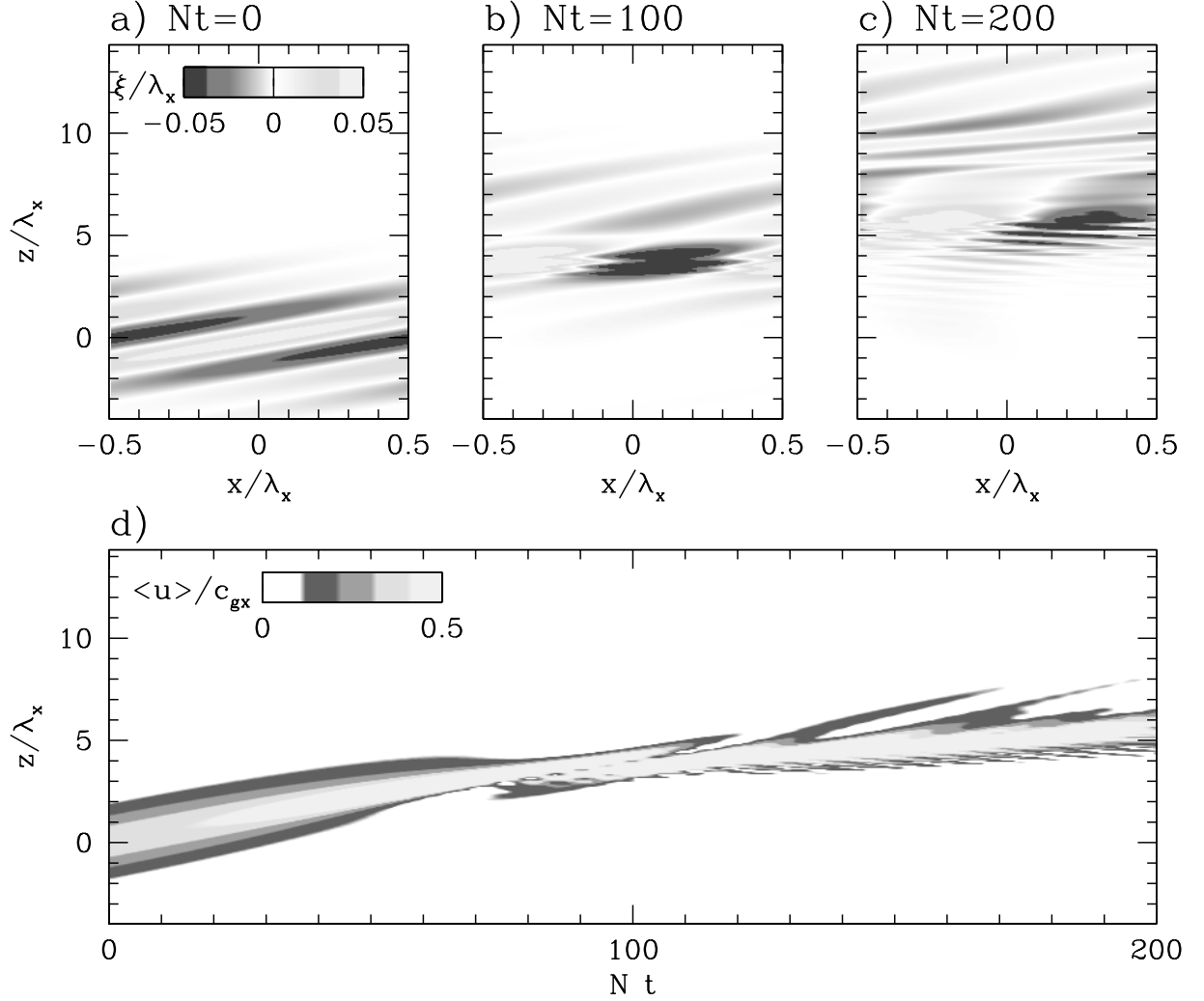
Figure 2: Simulation of moderately large amplitude Gaussian wavepacket prescribed initially with $A_\xi k_x = 0.30$, vertical wavenumber $k_z = -0.4k_x$, and width given by $\sigma k_x = 10$. Colour contours showing normalised vertical displacement associated with the wavepacket are shown at times a) $Nt = 0$, b) $Nt = 100$ ($t \simeq 16T_B$) and c) $Nt = 200$ ($t \simeq 32T_B$). The time evolution of the vertical profile of the normalised wave-induced mean flow is shown in d).

To re-emphasize, it is not the width but the slope of the amplitude envelope that determines the growth rate of the instability. This is demonstrated in Figure 4, which shows the evolution of a plateau-shaped wavepacket having the same effective width as the wavepacket shown in Fig. 3 but whose amplitude changes as rapidly on the leading and trailing flanks as the narrow Gaussian wavepacket shown in Fig. 2. Explicitly, the initial wavepacket is prescribed by (1) with $A_\xi/\lambda_x \simeq 0.048$ and $k_z = -0.4k_x$ as before, but here the amplitude envelope is given by (2) with $L_z = 30/k_x$ and $\sigma = 10/k_x$.

The initial growth in wavepacket amplitude occurs just as quickly as it does in the narrow large-

amplitude Gaussian wavepacket simulation, the increase taking place not at the wavepacket centre, where the amplitude is approximately constant, but at the leading flank.

The long-time development of the wavepacket is substantially more complex than in the narrow Gaussian case. After approximately 10 buoyancy periods self-acceleration slows the vertical advance of the leading edge of the wavepacket. Meanwhile, the amplitude of the waves below the leading edge begins to increase in amplitude, repeating the pattern of growth that occurred initially right at the leading edge.

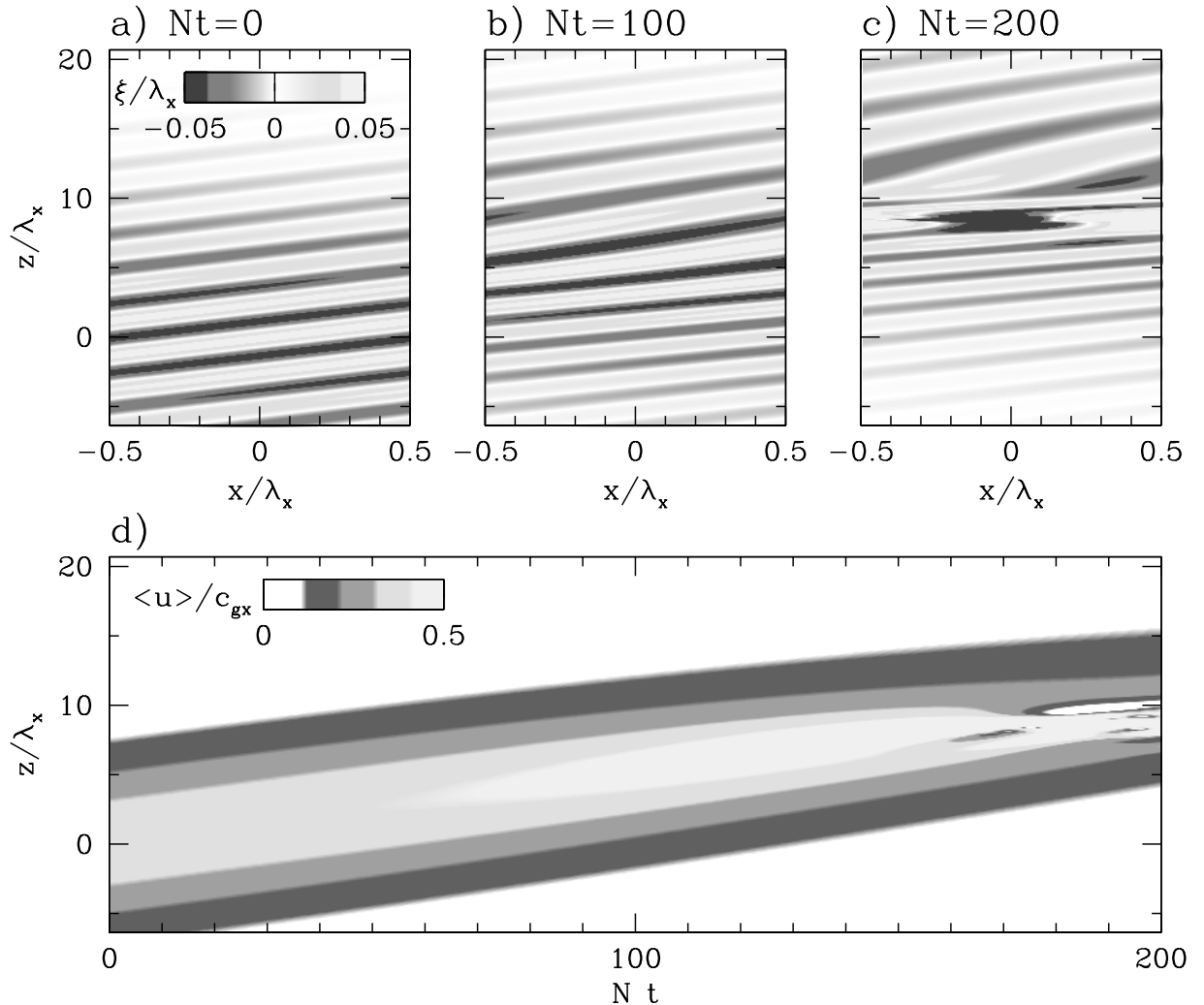After 16 buoyancy periods ($Nt = 100$), Fig. 4b

Figure 3: As in Fig. 2 but for a wide Gaussian wavepacket with $\sigma k_x = 10$.

illustrates the resulting structure of the waves. The leading edge has evolved to form a localized packet of waves with nearly vertical phase lines. Below this level, phase lines of the waves in the plateau region begin to tilt upward.

The process repeats over time with the wave-induced mean flow intrinsically changing the phase of the waves where-ever the amplitude envelope varies rapidly with height.

Parametric subharmonic instability is much more pronounced in this simulation, as might be expected because the span of the wavepacket over the plateau region is plane wave-like - locally it has constant amplitude. Self-acceleration is still the fastest mode of instability developing at the leading and trailing edges of the wavepacket, but once parametric instability has had time to grow (after approximately 20 buoyancy periods $Nt \simeq 125$) the wavepacket rapidly disperses with energy be-

ing transferred to waves with ever smaller vertical and horizontal scales. Except near the leading edge where a fraction of the initial wavepacket, however distorted, continues to progress upwards, the majority of the wavepacket has disintegrated after 32 buoyancy periods as a consequence of parametric subharmonic instability.

5. CONCLUSIONS

This process-study has been designed to illustrate the significance of interactions between moderately large amplitude nonhydrostatic internal waves and their induced mean flow (self-acceleration) in comparison with interactions between waves and their subharmonics (parametric subharmonic instability). The former are significant in particular for wavepackets having frequencies between $(2/3)^{1/2}N$ and N. The latter dominate for plane periodic waves and eventually de-
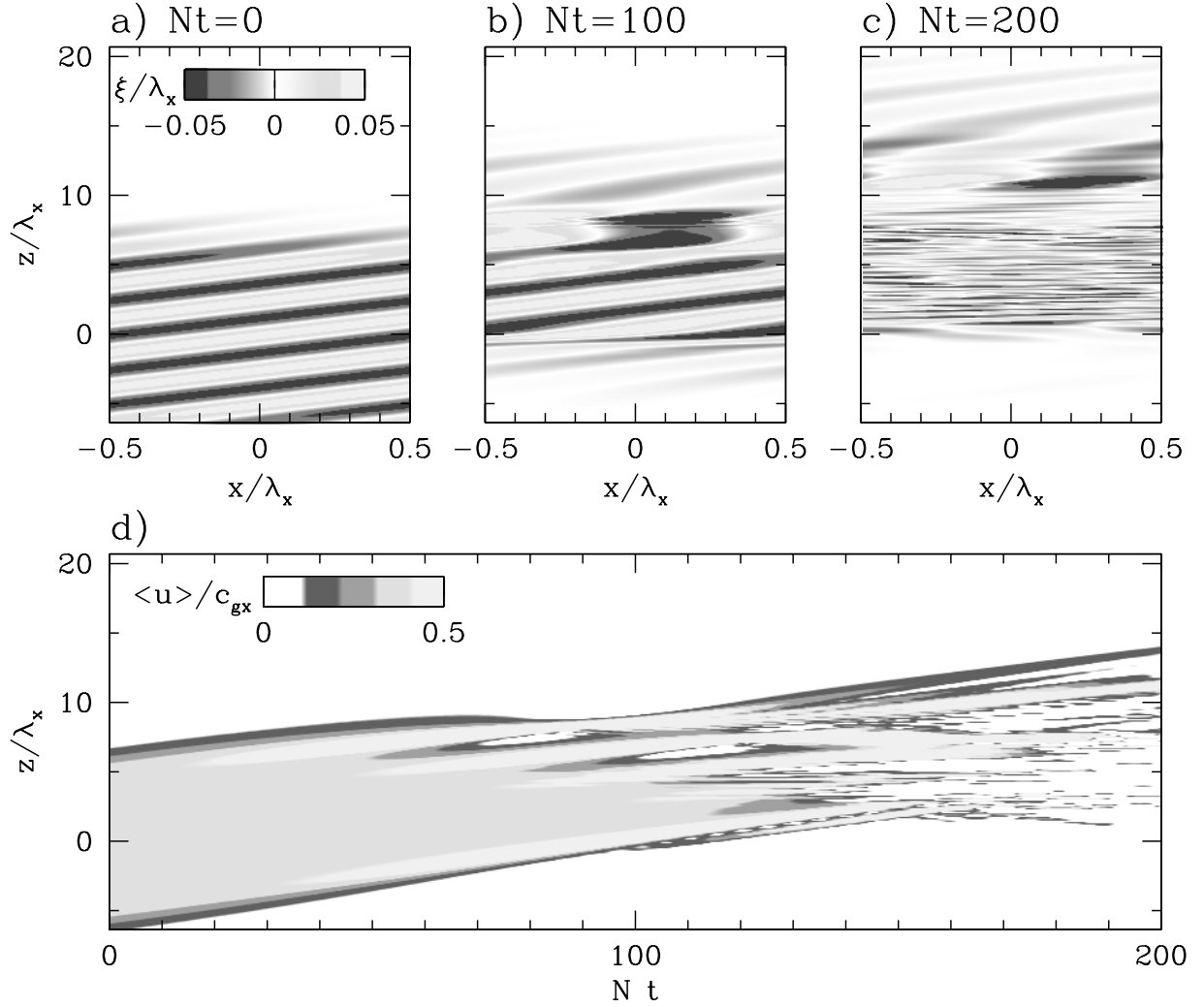
Figure 4: As in Fig. 2 but for a plateau-shaped wavepacket. Initially the constant amplitude region is prescribed by $L_z k_x = 30$ and the envelope decreases as a Gaussian on either flank with $\sigma k_x = 10$.

velop within wavepackets provided they are sufficiently wide and their amplitude is nearly constant over large depth.

Although nonlinear wave-wave interactions undoubtably influence the energy cascade from large to dissipative scales, idealized theoretical and numerical studies of parametric subharmonic instability have focused primarily upon plane periodic waves as the primary mechanism for internal wave instability in the absence of shear. Self-acceleration is an alternate instability mechanism that this study shows is dominant, at least during the initial evolution of nonhydrostatic (high-frequency) internal waves.

References

Sutherland, B. R. 2001. Finite-amplitude internal wavepacket dispersion and breaking. *J. Fluid Mech.*, 429:343–380.

Sutherland, B. R. 2005. Internal wave instability: Wave-wave vs wave-induced mean flow interactions. *J. Phys. Oceanogr.*, page submitted.